Int. J. Electrochem. Sci., 8 **(2013)** 17 - 26

International Journal of
ELECTROCHEMICAL
SCIENCE
www.electrochemsci.org

Controlling Physical and Chemical Bonding of Polypyrrole to Boron Doped Diamond by Surface Termination

Egor Ukraintsev[*1], *Alexander Kromka*[1], *Wiebke Janssen*[2], *Ken Haenen*[2], *Bohuslav Rezek*[1]

[1] Institute of Physics ASCR, Prague, Czech Republic
[2] Institute for Materials Research (IMO), Hasselt University & IMOMEC, IMEC vzw, Diepenbeek, Belgium
*E-mail: ukraints@fzu.cz

Received: 18 June 2012 / *Accepted:* 19 September 2012 / *Published:* 1 January 2013

To elucidate and to control polypyrrole (PPy) attachment to diamond we electrochemically grow PPy layers on hydrogen- and oxygen-terminated boron doped diamonds (BDD). Atomic force microscopy (AFM) shows that the PPy layers have similar morphology (15 nm features) and thickness (> 5 nm) on H- and O-BDD. To resolve type of PPy-diamond bonding, scanning electron microscopy (SEM) is used to compare intensity of secondary electron emission from original BDD regions and regions where PPy was grown and removed by AFM tip. The intensity on O-BDD remains unchanged. The intensity on H-BDD is lower than where the PPy was removed. This indicates chemical bonding (covalent) of PPy to H-BDD and physisorption (non-covalent) of PPy on O-BDD. This conclusion is corroborated by Kelvin force microscopy and by a model of energetic bands and electron affinity on the diamond surface.

Keywords: Electrochemical Growth, Polypyrrole, Boron Doped Diamond, Scanning Electron Microscopy, Kelvin Force Microscopy

1. INTRODUCTION

Polypyrrole (PPy) is a well-studied organic dye with conjugated system of electrons that is widely used in chemistry [1], optoelectronics [2, 3], and field-effect transistor (FET) devices [4]. Merging organic dyes with diamond has been proposed as a promising heterojunction for harvesting energy from light [5, 6]. PPy growth on intrinsic hydrogen-terminated monocrystalline diamond (H-MCD) was studied previously in detail, showing covalent grafting and consequently enhanced dissociation of excitons in such system [2, 7]. Unfortunately, undoped oxygen-terminated diamond is highly electrically resistive. Thus it does not enable electrochemical deposition to study possible specificity of hydrogen-pyrrole reaction and to compare properties of PPy on hydrogen- and oxygen-

terminated diamond, which can change the conformation of molecules [8] as well as electron transfer [9, 10]. Thus we used doping of the diamond to overcome the problem.

Doping by boron makes diamond a p-type semiconductor [11-13]. Doped diamond has many practical uses [14]. Boron doped diamond (BDD) electrodes are also well known due to their very high overpotential for both oxygen and hydrogen evolution [15]. Boron doping still preserves suitable biocompatibility [16] and chemical properties of diamond that enable covalent grafting of organic molecules [17]. As we will show, even low boron doping allows us to switch the surface atoms from hydrogen to oxygen without loss of conductivity. At low boron doping level the hydrogen terminated boron doped diamond (H-BDD) is conductive mainly due to presence of thin adsorbate layer on top on hydrogen terminated surface, so called surface transfer doping [18]. Yet also oxygen-terminated boron doped diamond (O-BDD) is still conductive due to an electron acceptor nature of boron atoms and hopping conductivity [19]. Low doping of diamond by boron was used to achieve reasonable conductivity of oxygen terminated diamond yet to minimize influence of boron for targeted optoelectronic applications, sensors, and FET devices.

It has been shown that the type of grafting between electrochemically grown material and substrate is important for such applications [6, 20, 21]. There are two types of grafting. Chemical bonding (grafting) means presence of chemical bond between grown material and substrate. Physical bonding (adsorption) means absence of chemical bond, but presence of non-covalent interactions like hydrogen bonds and van der Waals forces in general. Contact mode nanoshaving in atomic force microscopy (AFM) [22, 23] combined with surface potential measurements by Kelvin force microscopy (KFM) has been successfully applied to recognize covalent and non-covalent bonding of organic molecules to diamond [2, 6, 7, 20]. This is otherwise difficult in such all-carbon systems. Here we show that because scanning electron microscope (SEM) is sensitive to changes in surface terminations of diamond [24-26] it can be used to recognize creation of a covalent bond. We report SEM data supported by AFM, and KFM characterization, which indicate different grafting of PPy to hydrogen and oxygen terminated BDD and evidence that PPy bonding can be controlled by surface atoms on diamond.

2. EXPERIMENTAL PART

Boron doped diamond was grown on <100> Ib diamond substrates (Sumitomo) by plasma enhanced chemical vapor deposition (PECVD) in a home-made NIRIM type reactor. Diamond layer is grown in a mixture of 1% of methane (6 N) diluted in hydrogen (6 N) at a total pressure of 110 mbar, a microwave power of 500 W and a substrate temperature of ~1100°C. Boron doping is achieved using 180 ppb trimethylboron (TMB) diluted in hydrogen (200 ppm) [27]. From Hall experiments, the amount of charge carriers at room temperature was determined to be 2×10^{14} cm^{-3}, having a mobility of 1100 $cm^2V^{-1}s^{-1}$. The thickness of the doped layer is 1.6 μm. Boron doped diamond was hydrogen and oxygen terminated using plasma processes according to the published protocols [8].

For electrical connection, gold contacts were thermally evaporated (50 nm of Au) on the sample through the mask prepared by photolithography. Ma-P1215 resist (MicroChem) was used for

making the mask. For better contact stability, colloidal silver liquid (Pelco) was applied on top of the gold contacts. Distance between gold contacts was about 3 mm. The resistance of O-BDD sample before PPy growth was R_O~2.4 MOhm. The resistance of H-BDD sample was R_H~70-400 kOhm.

Fig. 1a show the setup used for electrochemical synthesis of PPy in microscopic spots (1 mm^2) on diamond. Microscopic deposition enables direct PPy growth on devices [28] as well as on relatively small monocrystalline diamond substrates. Such setup causes inhomogeneous electric field and current density distribution, which result in various thicknesses across larger area. Yet for microscopic regions (0.01 mm^2) the deposition is sufficiently uniform.

PPy was grown using a galvanostat Autolab PGSTAT302N (Metrohm). Constant currents 1 µA and 5 µA were applied for 150 s. The droplet volume was 0.1-0.3 µL. Pyrrole solution (240 mM Py and 100 mM NaCl in de-ionized water) was used. Distance between H/O-BDD (working electrode) and Pt wire (counter electrode and reference electrode) was about 100 µm. Fig. 1b illustrates the PPy growth curves on H/O-BDD. Those chrono-potentiometric curves are more or less flat except for the initial capacitive transient, i.e. the electrochemical cell potential was practically constant during the process. Larger applied current results in higher voltage. The voltage on O-BDD is higher than on H-BDD due to higher resistivity of O-BDD substrate.

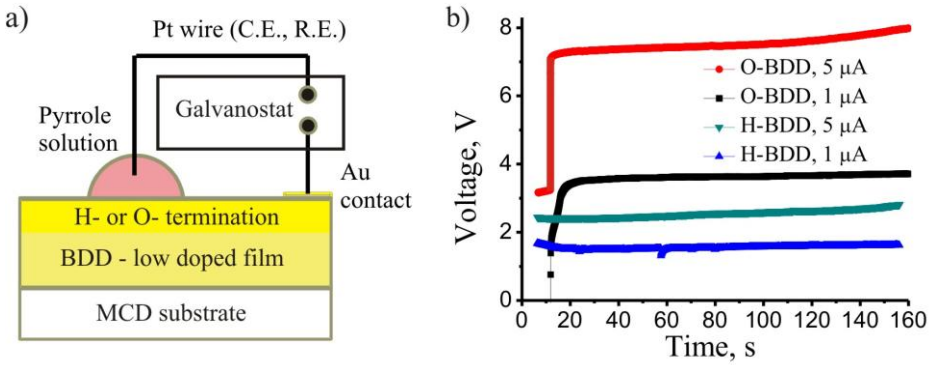

Figure 1. a) The scheme of microscopic setup used to grow PPy. b) Chrono-potentiometric characteristics of polypyrrole growth at 1 µA and 5 µA constant current on H- and O-terminated BDD surfaces.

AFM characterizations were performed using Multi75Al cantilevers (typical cantilever resonance frequency 75 kHz) in tapping, contact and KFM modes. The thickness of PPy layers and the threshold of PPy layer removal were measured using contact mode nanoshaving [22, 23]. AFM contact mode nanoshaving was used to remove PPy layer as well as contamination layer from diamond substrate prior KFM and SEM measurements. Note that even pristine diamond surface is typically contaminated by adsorbed hydrocarbon species. The adsorbate layer has thickness below 1 nm; however, it clearly influences SEM and KFM results [24].

To characterize secondary electron emission from the samples, field-emission scanning electron microscope (MIRA3, TESCAN) was operated with SE and InBeam detectors using 1 kV (in case of too high sample charging) and 5 kV acceleration voltage.

3. RESULTS

Typical morphology of PPy layers electrochemically synthesized on O- and H-BDD is presented in Fig. 2. Both diamond surfaces are covered with hillock-like features with average lateral size of 15 nm (determined by autocorrelation function [8]). The observed RMS surface roughness is 0.8 nm on O-BDD and 2.3 nm on H-BDD. PPy clusters with root mean square (RMS) roughness > 25 nm were observed to certain extent in the central parts of all PPy layers. This is because our microscopic setup leads to higher current density in the central part of deposited area. This leads to faster, diffusion limited growth, and consequently to PPy cluster formation there [29].

We used contact mode AFM nanoshaving [22, 23] to further characterize properties of the PPy layers. The procedure of the nanoshaving method is schematically presented in Fig. 2c. Based on this procedure, Fig. 2d shows the tapping mode AFM topography of PPy layer on O-BDD after the contact mode nanoshaving was performed in the central area. The applied force was in the range of 90-360 nN. Bare diamond surface is exposed in the central area where applied force $F \geq 180$ nN. This force thus corresponds to nanoshaving force threshold. Note that determination of the nanoshaving threshold worked well only on thin PPy layers (thickness < 30 nm). For thicker layers the force threshold was increasing over 1 μN and in some instances the PPy could not be removed by AFM at all. AFM and Raman measurements on H-MCD surface with PPy layer showed that PPy is completely removed by nanoshaving [30] and not step-by-step as in case of aryl diazonium salts [20]. Considering AFM nanoshaving results in Fig. 2d we assume that this is the same case here.

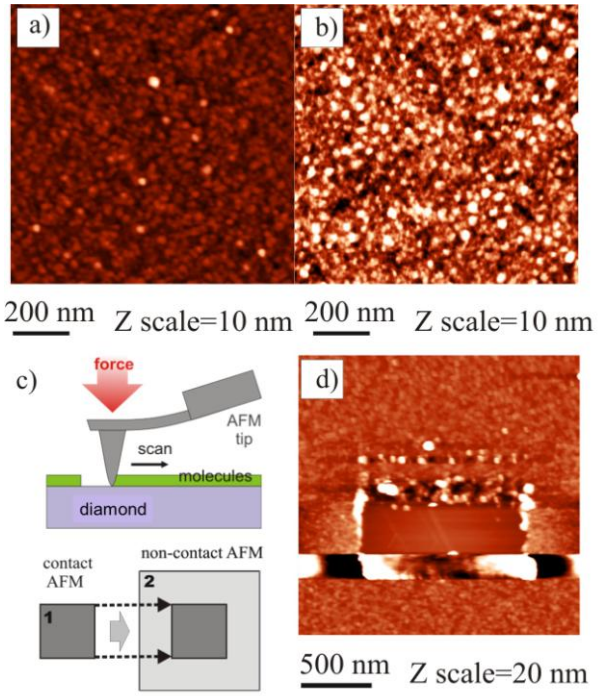

Figure 2. Topography AFM image obtained in tapping mode on thin (5 nm) PPy layer on a) O-BDD and b) H-BDD. c) The scheme of AFM contact mode nanoshaving by AFM tip. d) Topography AFM image obtained in tapping mode on thin (5 nm) PPy layer on O-BDD after contact mode nanoshaving in the central area (forces 90-360 nN, threshold 180 nN).

The nanoshaving method allows us to measure also PPy layer thickness. The thickness was about 5 nm on the edge of 1 μA spot and > 80 nm in the middle of 5 μA spot on O-BDD. The spot on H-BDD has inhomogeneous thickness 5 to 40 nm near the spot edge.

Fig. 3 shows SEM secondary electron images and intensity profiles obtained on the border between PPy layer and O-BDD or H-BDD, respectively. Contact mode nanoshaving was performed near the border on i) PPy on diamond and ii) original (pristine) diamond surface. The force of 300-500 nN was typically applied to completely remove PPy and adsorbate layers in the area of 5x5 μm^2. The SEM measurements reveal that in the case of O-BDD, the intensity of secondary electrons from original O-BDD surface and from the surface where PPy was synthesized and removed is the same (see Fig. 3a and 3b). In the case of H-BDD, the intensity of secondary electrons from original H-BDD surface is clearly lower than from the surface after PPy growth and removal (see Fig. 3c and 3d). Some charging of the samples was observed during SEM measurements. Possible reason is low sample conductivity. H-BDD surface is ~10 times and O-BDD surface is ~100 times less conductive than the H-MCD surface. However, the influence of charging on the results is negligible.

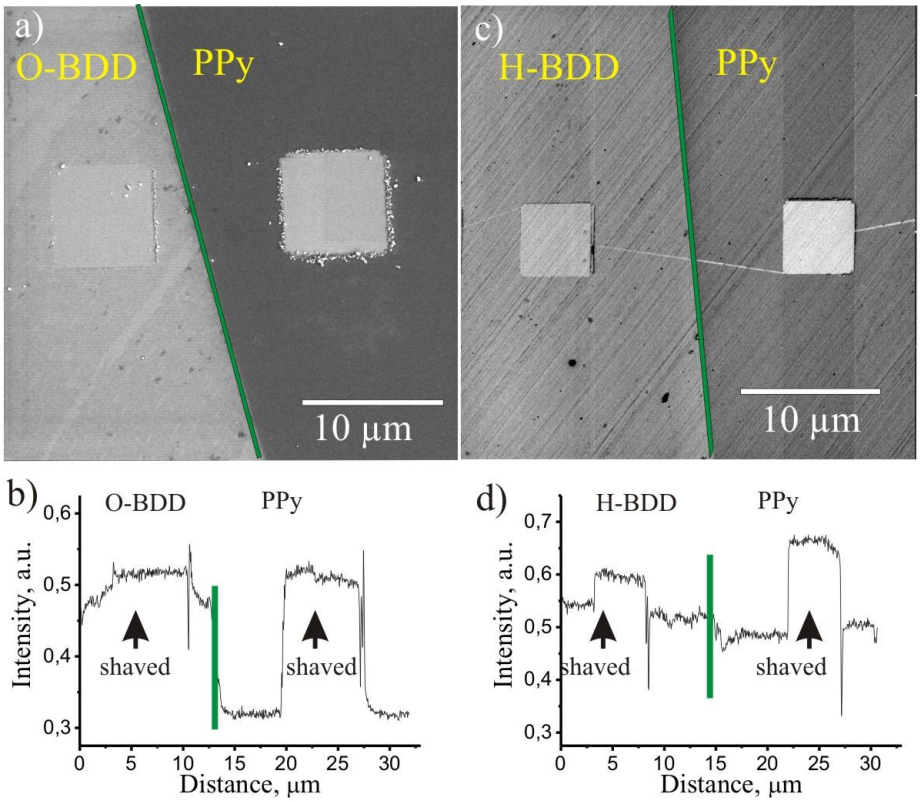

Figure 3. SEM image obtained on the border between thin (5 nm) PPy layer and O-BDD. The squares correspond to 7x7 μm^2 nanoshaved region. b) Corresponding intensity profile across O-BDD/PPy border and the nanoshaved squares. c) SEM image obtained on the border between PPy layer and H-BDD. The squares correspond to 5x5 μm^2 nanoshaved region. d) Corresponding intensity profile across H-BDD/PPy border and the nanoshaved squares. The green lines denote diamond/PPy border in the images and the profiles.

Fig. 4a shows SEM image and intensity profile obtained on the border between O-BDD and H-BDD. The intensity of secondary electrons on H-BDD is higher than on plasma oxidized O-BDD, in

agreement with the typical results on intrinsic diamond [8, 21]. Fig. 4b shows KFM surface potential image on the H-BDD/PPy border including nanoshaved regions on both parts. Some slope in the KFM image was observed. Yet one can still deduce that the diamond layer, where PPy was grown and removed, has about 40 mV higher surface potential than the pristine diamond layer if we account for the slope. This corresponds to lower work function in this case [24], in correlation with higher secondary electron intensity in SEM.

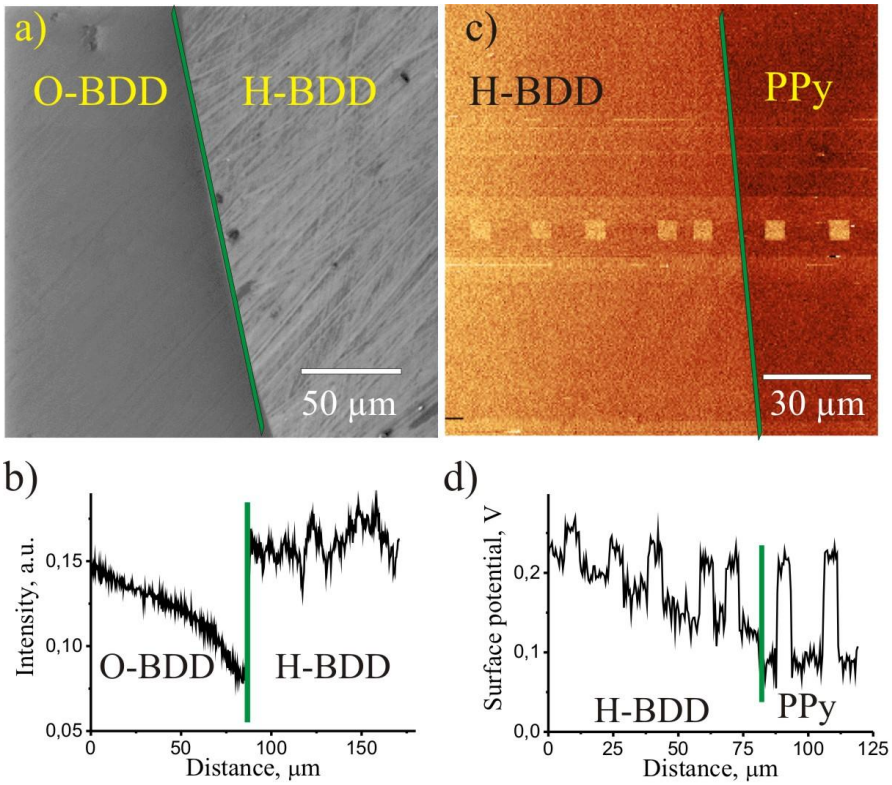

Figure 4. a) SEM image obtained on the border between O-BDD and H-BDD. b) Corresponding intensity profile across O/H border. c) KFM image obtained on the border of PPy layer and H-BDD. Small squares correspond to 5x5 μm^2 nanoshaved regions. d) Corresponding potential profile across H-BDD/PPy border and the nanoshaved squares. The green lines denote diamond/PPy border.

4. DISCUSSION

The AFM showed presence of deposited PPy layers on both H- and O-BDD. Thus the deposition is not selective based on diamond surface atoms. The AFM morphology of PPy on H- and O-BDD looks similar. The surface roughness is different; however, we observed that it depends more on the PPy layer thickness rather than on the substrate termination. So based on the AFM morphology data it is not possible to distinguish type of bonding between PPy and diamond with particular surface termination.

PPy removal forces of 180 nN during nanoshaving on O-BDD (Fig. 2d) were higher than typically found 40 nN for PPy [4] and other molecules [20] covalently grafted on H-MCD. This is probably due to certain cross-linking of thin PPy layers PPy on O-BDD. Thicker PPy layers required

even much higher forces (F > 1 μN) to be removed from both O-BDD and H-BDD. This can be explained by higher mechanical stability of the film and indicates crosslinking of the thick PPy layers irrespective of surface termination. However, that also means that on crosslinked layers the nanoshaving force threshold is not conclusive for evidencing grafting or for resolving bonding differences between PPy on H-BDD and O-BDD. Combination of the AFM nanoshaving with KFM (as reported previously [20]) or SEM (as reported newly here) is thus required to recognize the type of grafting.

The SEM data revealed the change of secondary electron intensity on H-BDD after PPy growth and removal. The contrast between H/O-BDD shown in Fig. 4a confirms that the higher intensity of secondary electrons on the nanoshaved PPy region compared to H-BDD (Fig. 3c) is not a measurement artifact. Note that replacing hydrogen by oxygen or carbon changes negative electron affinity towards positive and thus lower electron emission might be expected as in the case of intrinsic diamond [26]. However, there is also related change of surface band bending that plays significant role [24, 31].

Correlation between the surface modifications and intensity of secondary electrons in SEM can be explained by the following model which considers both the changes of electron affinity and surface Fermi level position and which is schematically shown in Fig. 5. Fig. 5 depicts energetic band configuration of pristine H-BDD before PPy growth, H-BDD after PPy growth and removal, and plasma oxidized O-BDD.

In the case of H-BDD the bands are bending upwards because hydrogen passivates the surface states on diamond and gives rise to negative electron affinity [31]. However, due to low boron doping, secondary electrons have to overcome relatively wide barrier. This is similar effect as observed on n-type diamond with H-terminated surfaces [31]. Note that we talk about secondary electrons generated in the bulk in our case, so it is not quite the same situation as in usual photoelectron emission experiments on intrinsic H-terminated diamond, which show no surface barrier [32].

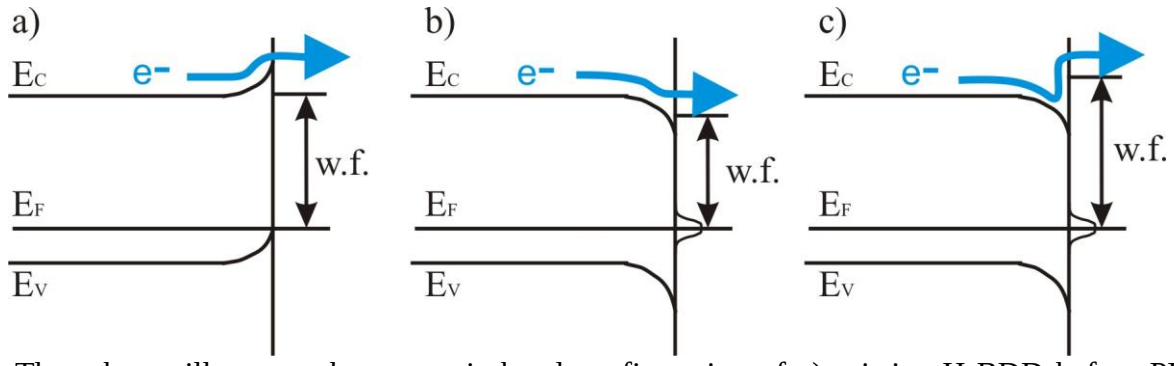

Figure 5. The scheme illustrates the energetic band configuration of a) pristine H-BDD before PPy growth, b) H-BDD after PPy growth and removal, c) plasma oxidized O-BDD. The symbols are explained as follows: Ec = conduction band minimum, Ef = Fermi level, Ev = valence band maximum, w.f. = work function.

In the two latter cases, surface states pin the Fermi level position (i.e. surface Fermi level changes) and surface band bending switches from upward to downward. At the same time, electron affinity increases towards more positive values as hydrogen is removed from the surface. In the case of

H-BDD after PPy growth and removal (Fig. 5b) the electron affinity increases only slightly so that it is below conduction band minimum in the bulk. This facilitates the easiest emission of electrons and the SEM intensity is the highest. On the other hand, on the plasma oxidized O-BDD the electron affinity becomes highly positive [32] which limits the electron emission (Fig. 5c). Thus SEM detects the lowest intensity of all three cases.

From the model it is obvious that different intensity of secondary electrons in SEM on the same diamond with different surface terminations reflects the change of surface atoms (hydrogen to oxygen or carbon) because they provide different electron affinity as well as surface Fermi level position (i.e. work function) [24, 26, 31, 33]. Assuming similar energetic position of surface states in Fig. 5b and 5c, electron affinity of diamond after PPy layer removal must be lower compared to O-BDD surface after plasma oxidation. Similarly, SEM was able to resolve trends in electron affinity of molecules on diamond [34]. Therefore, from the changes of secondary electron intensity we can deduce that hydrogen atoms were replaced and PPy was grafted (covalently bonded) to H-BDD during electrochemical deposition. In the case of O-BDD the intensity of secondary electrons on the nanoshaved PPy and nanoshaved O-BDD is the same. This evidences that no changes in work function occurred after PPy growth and removal. Thus only physical bond between PPy and O-BDD was formed.

The above conclusions and model based on SEM results are corroborated by and well correlated with KFM measurements. The diamond layer after PPy removal has higher surface potential than the diamond layer (after the slope correction). This is in agreement with higher secondary electron intensity in SEM and lower work function of the surface as suggested by the model. Such KFM contrast is opposite to the typical contrast observed on intrinsic H-MCD substrate after the growth and removal of PPy [2] as well as of other organic molecules [20]. This difference is obviously caused by the boron doping and it is well explained by the model in Fig. 5. Yet note that the slope in the surface potential map (Fig. 4c) indicates that the low boron doping may not be enough for clear interpretation of KFM data. SEM is thus able to resolve grafting (chemical bonding) vs. deposition (physisorption) even where KFM evaluation is difficult.

5. CONCLUSIONS

We showed that low boron doping makes BDD conductive enough for electrochemical growth of PPy on both hydrogen- and oxygen-terminated surfaces. The boron doping of diamond is a key factor which allow us to prove the absence of the chemical bond between the electrochemically grown PPy and O-BDD. SEM detected change of secondary electron emission on H-BDD surface after PPy growth and removal, from which covalent grafting of PPy to H-BDD via electrochemical synthesis was deduced based on the model of energetic bands and electron affinity. It is correlated well with the change of work function as observed by KFM. It is also in a good agreement with previously observed covalent grafting of PPy to H-terminated intrinsic diamond. On the other hand, no changes in SEM contrast were observed on O-BDD. Therefore, no chemical bond between PPy and diamond was formed in this case. Thus although the electrochemical growth of PPy was achieved on both H- and O-

BDD, the diamond surface atoms (H, O) determine the type of PPy-diamond bonding. Those may be useful features for diverse experiments and applications.

ACKNOWLEDGEMENTS
Technical support of Jitka Libertínová, Oleg Babchenko, Ondřej Rezek, Zdeňka Poláčková, and Vincent Mortet is gratefully appreciated. This research was financially supported by the project P108/12/G108 (GACR), P108/12/0996 (GAČR), the EU FP7 through Marie Curie ITN "MATCON" (PITN-GA-2009-238201) and the Collaborative Project ”MOLESOL” (No. 256617), and the Research Foundation Flanders (FWO) (G.0555.10N). This work occurred in frame of the LNSM infrastructure.

References

1. M. Yun, N.V. Myung, R.P. Vasquez, C. Lee, E. Menke and R.M. Penner, *Nano Letters*, 4 (2004) 419
2. B. Rezek, J. Čermák, A. Kromka, M. Ledinský and J. Kočka, *Diam. Relat. Mater.*, 18 (2009) 249
3. P. Galář, P. Malý, J. Čermák, B. Rezek, A. Kromka, *Int. J. Electrochem. Sci*,, under review
4. D.J. Shirale, M.A. Bangar, W. Chen, N.V. Myung and A. Mulchandani, *J Phys Chem C Nanomater Interfaces*, 114 (2010) 31, 13375
5. W.C. Poh, K.P. Loh, W. De Zhang, S. Triparthy, J.S.Ye and F.S. Sheu, *Langmuir*, 20 (2004) 5484
6. B. Rezek, J. Čermák, A. Kromka, M. Ledinský, P. Hubík, V. Cimrová and A. Fejfar, *Nanoscale Res. Lett.*, 6 (2011) 238
7. J. Čermák, A. Kromka, M. Ledinský and B. Rezek, *Diam. Relat. Mater.*, 18 (2009) 800
8. B. Rezek, L. Michalíková, E. Ukraintsev, A. Kromka, M. Kalbacova, *Sensors*, 9 (2009) 3549
9. A. Kromka, M. Davydova, B. Rezek, M. Vanecek, M. Stuchlik, P. Exnar, *Diam. Relat. Mater.*, 19 (2010) 196
10. S. Stehlik, T. Izak, A. Kromka, B. Dolenský, M. Havlík, B. Rezek, *ACS Appl. Mater. Interfaces*, 4 (2012) 3860
11. W. Haenni, P. Rychen, M. Fryda and C. Comninellis: *Thin-Film Diamond B*, C. E. Nebel, Editor, Academic Press, Semiconductors and Semimetals series, Elsevier, (2004), 149
12. J. Mort, D. Kuhman, M. Machonkin, M. Morgan, F. Jansen, K. Okumura, Y. M. LeGrice, and R. J. Nemanich, *Appl. Phys. Lett.*, 55, (1989) 112113 S.-G. Ri, H. Kato, M. Ogura, H. Watanabe, T. Makino, S. Yamasaki, H. Okushi, *J. Crystal Growth*, 299 2 (2007) 235
14. A. Kraft, Int. *J. Electrochem. Sci.*, 2 (2007) 355
15. M. Swain, A.B. Anderson and J.C. Angus: *MRS Bulletin*, (1998) 56
16. L. Grausova, A. Kromka, Z. Burdikova, A. Eckhardt, J. Vacik, B. Rezek, K. Haenen, V. Lisa, L. Bacakova, *PLoS ONE*, 6 (2011) e20943
17. D. Shin, N. Tokuda, B. Rezek, C. E. Nebel, *Electrochem. Commun.*, 8 (2006) 844
18. J. Ristein, *Appl. Phys. A*, 82 (2006) 377
19. J. Pernot, P.N. Volpe, F. Omnès, P. Muret, V. Mortet, K. Haenen, T. Teraji, *Phys. Rev. B*, 81/20 (2010), 205203.
20. B. Rezek, D. Shin, H. Uetsuka and C. E. Nebel, *Phys. stat. sol. (a)*, 204 (2007) 2888
21. W. Yang, O. Auciello, J.E. Butler, W. Cai, J.A. Carlisle, J. Gerbi, D.M. Gruen, T. Knickerbocker, T.L. Lasseter, J.N. Russell Jr., L.M. Smith and R.J. Hamers, *Nature Materials*, 1 (2002) 253
22. B. Rezek, D. Shin and C.E. Nebel, *Langmuir*, 23 (2007) 7626
23. E. Ukraintsev, B. Rezek, A. Kromka, A. Brož and M. Kalbacova, *Phys. stat. sol. (b)*, 246 (2009) 2832
24. B. Rezek and C. E. Nebel, *Diam. Relat. Mater.*, 14 (2005) 466

25. M. Tachiki, Y. Kaibara, Y. Sumikawa, M. Shigeno, H. Kanazawa, T. Banno, K.S. Song, H. Umezawa, H. Kawarada, *Surf. Science*, 581, (2005) 207
26. B. Rezek, C. Sauerer, C. E. Nebel, M. Stutzmann, J. Ristein, L. Ley, E. Snidero, P. Bergonzo, *Appl. Phys. Lett.*, 82 (2003) 2266
27. V. Mortet, M. Daenen, T. Teraji, A. Lazea, V. Vorlicek, J.D'Haen, K. Haenen and M.D'Olieslaeger, *Diam. Relat. Mater.*, 17 (2008) 1330
28. J. Čermák, B. Rezek, P. Hubík, J.J. Mareš, A. Fejfar and A. Kromka, *Diam. Relat. Mater.*, 19 (2010) 174
29. J. Kaufman, O.R. Melroy, F.F. Abraham and A.I. Nazzal, *Solid State Communications*, 60, 9 (1986) 757
30. J. Čermák, B. Rezek, A. Kromka, M. Ledinský and J. Kočka, *Diam. Relat. Mater.*, 18 (2009) 1098
31. D. Takeuchi, H. Kato, G. S. Ri, T. Yamada, P. R. Vinod D. Hwang, C. E. Nebel, H. Okushi and S. Yamasaki, *Appl. Phys. Lett.*, 86 (2005) 152103
32. D. Takeuchi, S.-G. Ri, H. Kato, C.E. Nebel and S. Yamasaki, *Diam. Relat. Mater.*, 15 (2006) 698
33. M.C. Salvadori, W.W.R. Araújo, F.S. Teixeira, M. Cattani, A. Pasquarelli, E.M. Oks and I.G. Brown, *Diam. Relat. Mater.*, 19 (2010) 324
34. X. Wang, P.E. Colavita, K.M. Metz, J. E. Butler and R. J. Hamers, *Langmuir*, 23 (2007) 11623